A Liposome-Micelle-Hybrid (LMH) Oral Delivery System for Poorly Water-Soluble Drugs: Enhancing Solubilisation and Intestinal Transport

European Journal of Pharmaceutics and Biopharmaceutics

A Liposome-Micelle-Hybrid (LMH) Oral Delivery System for Poorly Water-Soluble Drugs: Enhancing Solubilisation and Intestinal Transport

--Manuscript Draft--

Manuscript Number:	
Article Type:	Research Paper
Keywords:	Lovastatin; Liposomes; Micelles; Liposome-micelle hybrid; LMH, Caco-2 cells; Permeability; P-gp; Bioavailability.
Corresponding Author:	Clive Prestidge University of South Australia Adelaide, South Australia AUSTRALIA
First Author:	Bilquis Romana
Order of Authors:	Bilquis Romana
	Md Musfizur Hassan
	Fabio Sonvico
	Gabriela Garrastazu Pereira
	Alex F Mason
	Pall Thodarson
	Kristen E Bremmell
	Timothy J Barnes
	Clive Prestidge
Abstract:	A novel liposome-micelle-hybrid (LMH) carrier system was developed as a superior oral drug delivery platform compared to conventional liposome or micelle formulations. The optimal LMH system was engineered by encapsulating TPGS micelles in the aqueous core of liposomes and its efficacy for oral delivery was demonstrated using lovastatin (LOV) as a model poorly soluble drug with P-gp (permeability glycoprotein) limited intestinal absorption. LOV-LMH was characterised as unilamellar, spherical vesicles encapsulating micellar structures within the interior aqueous core and showing an average diameter below 200 nm. LMH demonstrated enhanced drug loading, water apparent solubility and extended/controlled release of LOV compared to conventional liposomes and micelles. LMH exhibited enhanced LOV absorption and transportation in a Caco-2 cell monolayer model of the intestine by inhibiting the P-gp transporter system. The LMH system is a promising novel oral delivery approach for enhancing bioavailability of poorly water-soluble drugs, especially those presenting P-gp effluxes limited absorption.
Suggested Reviewers:	Yvonne Perrie University of Strathclyde yvonne.perrie@strath.ac.uk
	Thomas Rades Kobenhavns Universitet thomas.rades@sund.ku.dk
	Benjamin Boyd Monash Institute of Pharmaceutical Sciences ben.boyd@monash.edu
	Christel Bergstrom Uppsala Universitet Christel.Bergstrom@farmaci.uu.se
	Brendan Griffin University College Cork National University of Ireland Brendan.Griffin@ucc.ie

Opposed Reviewers:	

University of South Australia

Professor Clive Prestidge
UniSA: Clinical and Health Sciences
University of South Australia
Cancer Research Institute
Adelaide, South Australia, Australia
P: +61 8 830 22438
E: clive.prestidge@unisa.edu.au

Professor Goepferich
Editor-in-Chief
European Journal of Pharmaceutics and Biopharmaceutics

23rd April, 2020

UniSA: Clinical and Health Sciences

Adelaide
South Australia 5000

GPO Box 2471
Adelaide
South Australia 5001

t +61 8 8302 2391
f +61 8 8302 2389

www.unisa.edu.au

CRICOS Provider Number 00121B

Dear Professor Goepferich,

Please find enclosed our manuscript entitled "A Liposome-Micelle-Hybrid (LMH) Oral Delivery System for Poorly Water-Soluble Drugs: Enhancing Solubilisation and Intestinal Transport" by Bilquis Romana *et al.* for consideration as an original contribution in the European Journal of Pharmaceutics and Biopharmaceutics.

LMH are a novel hybrid drug carrier system and to our knowledge have not been reported for oral delivery applications. Specifically, here we explore the synergy of encapsulating micelles into the core of liposomes for delivery of the poorly soluble drug, Lovastatin. Comprehensive studies were undertaken to evaluate the performance of the system during *in vitro* dissolution and transport studies. We report on the fabrication and physicochemical characterisation of the liposome-micelle hybrid (LMH) carrier system. LMH displayed enhanced drug loading and extended controlled release of Lovastatin compared to the individual liposomes or micelles. Enhanced transportation across Caco-2 cell monolayers was also achieved. The research demonstrates the synergy that can be achieved through combining micelles and liposomes into one nanoparticulate drug carrier system.

All authors have contributed to the design and article preparation of this manuscript. This manuscript has not been published and is not under consideration for publication elsewhere.

We hope that this manuscript is received as an important piece of work highly relevant to the scope of the European Journal of Pharmaceutics and Biopharmaceutics.

Yours sincerely,

Clive A. Prestidge
Professor of Pharmaceutical Science

Graphical Abstract

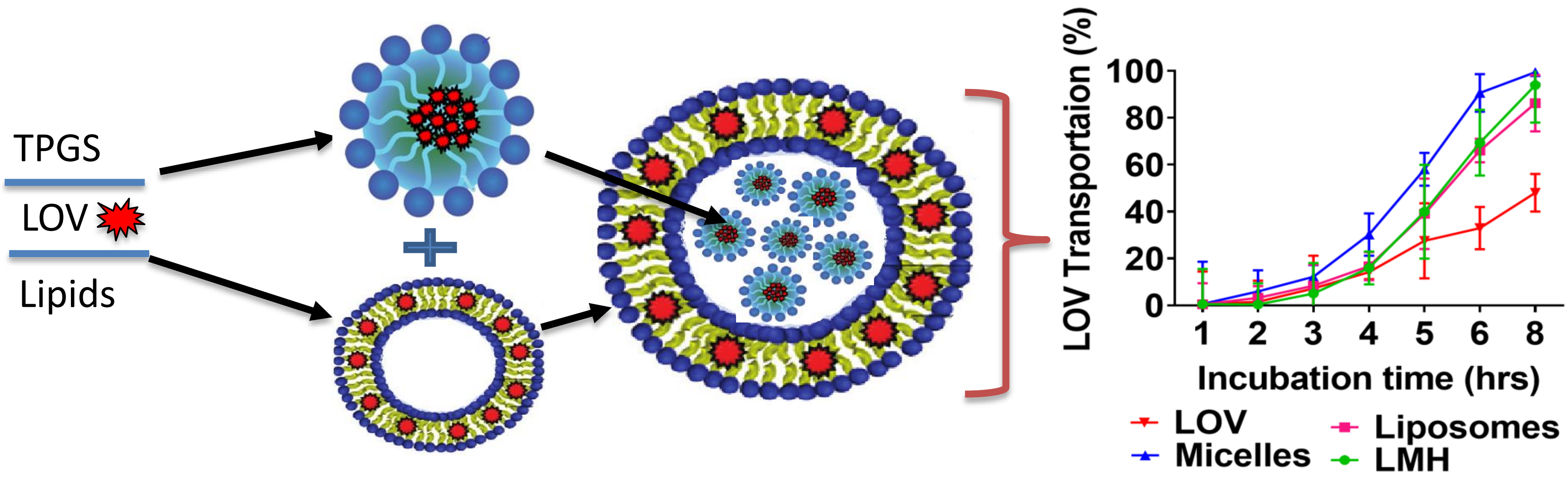

A Liposome-Micelle-Hybrid (LMH) Oral Delivery System for Poorly Water-Soluble Drugs: Enhancing Solubilisation and Intestinal Transport

Bilquis Romana[1,3], Md. Musfizur Hassan[1§], Fabio Sonvico[2,a], Gabriela Garrastazu Pereira[2b], Alex F Mason[1], Pall Thordarson[1], Kristen E. Bremmell[3], Timothy J. Barnes[3], Clive A Prestidge[3,4,*].

[1] School of Chemistry, the Australian Centre for Nanomedicine and The ARC Centre of Excellence in Convergent Bio-Nano Science and Technology, the University of New South Wales, Sydney, NSW 2052, Australia

[2]Discipline of Pharmacy, Graduate School of Health, University of Technology Sydney, Sydney, NSW 2007, Australia

[3]University of South Australia, Clinical and Health Sciences, Adelaide, South Australia 5000, Australia

[4]ARC Centre of Excellence in Convergent Bio-Nano Science and Technology, University of South Australia, Mawson Lakes Campus, Mawson Lakes 5095, Australia

[§]Contributed equally to the 1st author

[a]presently at the Department of Food and Drug, University of Parma, Parco Area delle Scienze 27/a, 43124 Parma, Italy

[b]presently at Faculdade de Farmacia, Universidade de Lisboa, Lisboa e Regiao, Portugal

*Corresponding author: Clive A. Prestidge; email: clive.prestidge@unisa.edu.au

Abstract

A novel liposome-micelle-hybrid (LMH) carrier system was developed as a superior oral drug delivery platform compared to conventional liposome or micelle formulations. The optimal LMH system was engineered by encapsulating TPGS micelles in the aqueous core of liposomes and its efficacy for oral delivery was demonstrated using lovastatin (LOV) as a model poorly soluble drug with P-gp (permeability glycoprotein) limited intestinal absorption. LOV-LMH was characterised as unilamellar, spherical vesicles encapsulating micellar structures within the interior aqueous core and showing an average diameter below 200 nm. LMH demonstrated enhanced drug loading, water apparent solubility and extended/controlled release of LOV compared to conventional liposomes and micelles. LMH exhibited enhanced LOV absorption and transportation in a Caco-2 cell monolayer model of the intestine by inhibiting the P-gp transporter system. The LMH system is a promising novel oral delivery approach for enhancing bioavailability of poorly water-soluble drugs, especially those presenting P-gp effluxes limited absorption.

Keywords: Lovastatin, Liposomes, Micelles, LMH, Caco-2 cells, Permeability, P-gp, Bioavailability.

1. Introduction

Poorly water-soluble drug candidates are often the output of contemporary drug discovery programs and present formulators considerable technical challenges and difficulties. These include low encapsulation efficiency, poor drug release kinetics, drug leakage, aggregation, poor biodistribution, toxicity and potential manufacturing issues [1, 2, 3]. LOV is a highly lipophilic (logP 4.26) Biopharmaceutical Classification System (BCS) class II drug (high permeability and low solubility) with limited aqueous solubility (0.4 mg/L), and low oral bioavailability, typically below 5% [4]. It is one of the most widely used cholesterol-lowering drugs as it irreversibly inhibits the enzymatic conversion of hydroxymethyl glutaryl coenzyme A (HMG-CoA) to mevalonate [5] which is critical to the biosynthesis of cholesterol [6]. Due to poor water solubility and high lipophilicity, LOV undergoes extensive pre-systemic first-pass metabolism in the liver, resulting in low and variable bioavailability, with only 30% of the oral dose absorbed [7, 8]. In fact, the low bioavailability of LOV is attributed to multiple aspects: (1) limited aqueous solubility and poor dissolution, (2) high affinity to intestinal and liver cytochrome P450 metabolic enzymes and (3) efflux due to the multidrug resistance protein 1 (MDR1) membrane transporter also known as P glycoprotein (P-gp) [9]. P-gp is expressed in the intestinal epithelium and liver cells, where it has been shown to limit the oral absorption of LOV through efflux from the intestinal mucosa to gut lumen against a concentration gradient [10, 11].

There is ongoing interest in overcoming LOV's *in vivo* susceptibility to P-gp mediated efflux [8] by utilising a variety of nano and [12] lipid-based [13] drug delivery systems (DDS) including self-emulsifing formulations [14] and liposomes [15]. For example, Sarangi *et al.* developed a lovastatin-solid lipid nanoparticle (LOV-SLN) formulation with a drug loading of 17.7% and encapsulation efficiency of 71%, that demonstrated a 1.72-fold increase in C_{max} and a 269% increase in bioavailability compared to a LOV suspension when orally administered to a rabbit model [16]. Similarly, Yanamandra *et al.* formulated a lovastatin-proliposome with a 3-fold increase in C_{max} and a 162% increase in bioavailability compared to pure LOV upon oral dosing of Sprague Dawley rats [15].

Micelles and liposomes have gained significant attention in the field of oral administration as they can improve the bioavailability of orally administered hydrophobic drugs [17]. They can also protect encapsulated drugs against degradation by enzymes in the gastrointestinal tract and reduce the first-pass effect. Despite these advantages, micelle and liposome-based drug delivery systems present numerous formulation challenges. For micellar systems, these include their inadequate drug loading capacity, poor physical stability in physiological environment that may lead to an undesirable rapid drug release *in vivo* and insufficient binding and uptake by cells. For liposomes, their inherent instability is a significant challenge in addition to their low drug encapsulation efficiency, poor storage stability (e.g. aggregation, sedimentation, fusion and oxidation) and rapid leakage of encapsulated drugs in the presence of biologic fluids [18].

Previous research has shown that lipid-polymer hybrid nanoparticles have some unique advantages such as high drug encapsulation yield, sustained drug release profiles, excellent serum stability, and potential for differential targeting of cells or tissues, while excluding some of their intrinsic limitations, thereby holding great promise as delivery vehicles for various medical applications [19, 20, 21, 22]. However, the assembly of multiple materials and/or agents into one nanoparticle (NP) formulation is often challenging and requires optimization to achieve synergy from the individual NP components.

Here, a novel hybrid nano-carrier system composed of micelles encapsulated within liposomes, i.e. liposome-micelle-hybrid (LMH), is reported as a robust drug delivery platform able to combine the unique strengths of each component. The encapsulated micelles control drug release, while the liposomal carrier increases the loading efficiency, protects the drug from first pass effect, and plays a role in mediating P-gp efflux. This synergistic and hierarchical structure represents an interesting development in oral drug delivery of hydrophobic drugs.

2. Materials and methods

2.1 Materials

TPGS (d-α-tocopheryl polyethylene glycol 1000 succinate) was purchased from Antares Health Product, INC. Jonesborough, TN, USA. Phosphatidylcholine (PC), cholesterol (CHO) (99%, MW 386.65 Da), phosphate buffer solution (PBS) tablets, HPLC grade acetonitrile, methanol and analytical grade chloroform and ethanol were purchased from Sigma-Aldrich St. Louis, MO, USA). The 1,2-distearoyl-sn-glycero-3-phospho-1'-rac-glycerol sodium-salt (DSPGNa with C18:0, >99%, MW 801.058 Da) was purchased from Avanti Polar Lipids (Alabaster, AB, USA). Lovastatin (LOV crystalline powder, 98%) was obtained from International Laboratory (South San Francisco, CA, USA). The reagents NaOH, NaCl, H_3PO_4, Tween 20, PEG-400 were ordered from Ajax Chemicals (Scoresby, VIC, Australia).

Polycarbonate Transwell inserts (0.4 µm pores and a surface area of 0.7 cm^2, 24-well polystyrene plates with inserts and lids) were purchased from Millipore Corporation Ltd., (Bedford, MA, USA). Dulbecco's modified eagle`s medium (DMEM), 10% fetal bovine serum (FBS) and transport buffer Hank's balanced salt solution (HBSS) were purchased from Gibco Life Technologies (Camarillo, CA, USA). Alamar Blue® was purchased from ThermoFisher (Waltham, MA, USA). Trypsin 0.25% w/v in PBS, dimethyl sulfoxide (DMSO), 4-(2-hydroxyethyl)-1-piperazineethanesulfonic acid (HEPES) and permeability marker Lucifer Yellow (LY) solution were also purchased from Sigma-Aldrich (St. Louis, MO, USA). Human epithelial colorectal adenocarcinoma cell line Caco-2 was kindly donated by the School of Medical Science, University of Sydney (Sydney, NSW, Australia). Ultrapure MilliQ water was used for all experiments and generated by a Milli-Q® Ultrapure water system connected with Q-Gard® purification cartridge and Quantum® EX polishing cartridge.

2.2 Formulation of LOV loaded micelles

The preparation method used for micelles was a modification of the direct dissolution and solvent evaporation method [23]. TPGS (100-800 mg) was weighed into a round bottom flask and dissolved in chloroform (10 mL) by gentle hand shaking to form a clear solution. A 1 mg/mL LOV solution in chloroform (10 mL) was added to TPGS solution. The TPGS-drug solution was subjected to vacuum evaporation in a rotary evaporator to eliminate chloroform (Rotavapor R-124, Büchi, Flawill, Switzerland operated 80 rpm and room temperature), and after 2-3 h, a thin polymer-drug film was formed. The thin film was hydrated with 10 mL of 1 mM freshly prepared and filtered (0.22 µm Syringe Filter PTFE 13 mm, Grace, IL, USA) NaCl solution and then subjected to sonication for 30 min (GT Ultrasonic Bath, Model VGT-1730QTD) to form micelles. A clear dispersion of drug-loaded micelles was then obtained. Any precipitated drug particles formed in the process were separated by centrifugation at 10,000 rpm for 20 min (100605 x g, The Avanti JXN-30).

2.3 Formulation of liposomes

Liposomes were prepared by a thin-film hydration method previously described by Bangham *et al.* [24], from PC, CHO and DSPGNa (molar ratio of 7:3:2), while LOV was incorporated into the formulations using a 2:1 molar ratio (LOV:formulation). The lipids and LOV were weighed, mixed, and dissolved in a mixture of methanol-chloroform-water (10 mL) at a ratio of 1:5:0.1 in a round bottom flask by gentle hand shaking and sonication (1-2 min) to form a clear solution. The round-bottom flask was connected to a rotary evaporator (Rotavapor R-124, Büchi, Flawill, Switzerland; water bath B-480, Xiamen, Fujian, China). The excipient-solvent mixture was evaporated under vacuum for 3 h, with gentle rotation (60 rpm) to prepare uniform drug-lipid films upon complete evaporation of the organic solvents at 60°C, which is above the phase transition temperature (T_c) of the lipids (55°C) [25]. The thin lipid film was dried for an additional hour under N_2 gas before leaving the flask open in a fume hood overnight in order to ensure complete removal of the solvent.

The resultant drug-lipid film was hydrated with 1 mM NaCl for 2 h in a water bath with controlled temperature (60 °C) with constant rotation at slow speed. The solution of 1 mM NaCl was used to provide a simple background electrolyte concentration (to enable determination of zeta potential) as reported in literature [26]. The hydrated solution was subsequently sonicated in an ice bath for 10 min. The ice bath was used to improve the rigidity of the obtained liposomes [27]. The drug-loaded liposomes (pellets) were separated from the unencapsulated free drug (supernatant) by ultracentrifugation at 32,000 rpm (114,688 x g, Avanti JXN-30). The liposome pellets were re-suspended in 1 mM NaCl solution, extruded 8–10 times through polycarbonate filters with 400-800 nm pore diameter to obtain highly monodispersed (PDI < 0.25) and unilamellar liposomes.

2.4 Formulation of liposome-micelle-hybrids

To fabricate the LMH systems, drug loaded TPGS micelles were prepared and subsequently mixed at the composition used in the thin film evaporation (TFH) method to obtain liposomes. Briefly, the method is equivalent to conventional liposome preparation, however the thin drug-lipid film was hydrated with the pre-formed LOV micelle dispersion instead of the 1 mM NaCl solution. After rehydration, the suspension was sonicated and ultracentrifuged**.** Drug present in the pellet and supernatant was analysed separately as described below. LOV in the pellet was considered as encapsulated within the LMH, while LOV in the supernatant was considered as unencapsulated drug, most likely present in free micelles.

LOV was loaded into LMH, both in the bilayer and micelles. Additionally, two control formulations were obtained i.e. LMH_{IN}: a blank lipid bilayer and LOV-loaded micellar inner core and LMH_{EX}: a LOV-loaded lipid bilayer and an aqueous inner core containing blank micelles. The LMH were freeze dried with cryoprotectant sucrose (Martin Christ, D-37520) at -50 ℃ and 0.001 bar in empty weight vials to obtain their final weight.

2.5 HPLC method for lovastatin assay

The amount of LOV in LMH formulations was analysed using an HPLC system (Shimadzu, Scientific Instruments, Kyoto, Japan) equipped with a UV-detector **(**PD-M2OA) set at 237 nm with a Phenomenex Hyper clone 5 µm-ODS C18 column (125 x 4.0 mm, 120 Å, Phenomenex, Torrance, CA, USA).

The mobile phase was a mixture of 65% v/v acetonitrile and 35% v/v 10 mM phosphoric acid aqueous solution. The solution pH was adjusted to 3.0 with 1 M NaOH solution. The mobile phase was degassed by ultra-sonication for 30 min before use and was not allowed to recirculate during the analysis. The samples were injected at a volume of 20 µL at ambient temperature. An isocratic method was applied with a flow rate of 1.5 mL/min. A series of working solutions with concentrations ranging from 0.1 to 100 µg/mL were used to generate the calibration curve (n = 3) by plotting the chromatographic peak area versus LOV concentrations (R^2=0.9998). The limit of quantification (LOQ) value was 0.1 µg/mL. The precision and accuracy for both intra and inter-day analyses were within the acceptable analytical limits (*i.e.* <10%). The specificity and reproducibility of the assay were within a 102-108% range. Repeated analysis showed excellent precision (<3%) in the peak area results. Therefore, the selected HPLC method was considered suitable for LOV quantification. All analytes were diluted suitably to meet the calibration concentration range prior to analysis.

2.6 Encapsulation efficiency and drug loading

LOV content in LMH and other formulations was determined by diluting 100 µL of each formulation with 900 µL of methanol followed by vortexing and sonication to breakdown the carriers. All samples were centrifuged prior to analysis and the supernatant was analysed for LOV using HPLC. The percentage ratio between the amount of drug encapsulated in nanocarriers and the initial drug concentration was calculated as an encapsulation efficiency (*EE*%) and drug loading (*DL%*) of LOV in the nanocarriers was expressed as the amount of entrapped drug in the nanocarriers and the total weight of nanocarriers.

2.7 Characterisation

2.7.1 Particle diameter and zeta potential

The average particle diameter (Z-average), size distribution (polydispersity index, PDI) and zeta potential of the LMH and other formulations were measured by Dynamic Light Scattering (DLS) and Phase Analysis Light Scattering (PALS) techniques using a Zetasizer Nano ZSP (Malvern analytical, Malvern, UK). The micelle dispersions were analysed directly, while the liposomes or the LMH systems were diluted 100 times with Milli-Q water prior to size and zeta potential analysis. For each sample, the size was measured 3 times with 6 runs of 4 min (1 min for equilibrium and 3 min for measurement) at 25 ºC and the material RI was set at 1.59.

2.7.2 Morphology

All cryo-TEM work was carried out in the Electron Microscope Unit at the Mark Wainwright Analytical Centre of the University of New South Wales (Sydney, NSW, Australia). Aqueous samples were vitrified using an EM GP vitrification robot (Leica Microsystems, Germany), using the following method. The aqueous sample (6 μL) was pipetted onto 300 mesh copper grids with a lacey formvar film (GSCu300FL-50, ProSciTech, Australia). The sample droplet was allowed to equilibrate for 30 seconds at room temperature and 90% relative humidity, before being blotted from one side for few seconds. The blotted grid was subsequently plunged into liquid ethane at -174 °C, excess ethane was blotted away with a piece of pre-cooled filter paper, and the vitrified grid stored in liquid nitrogen. Vitrified grids were imaged using a Gatan 626 cryo holder, in a Technai G2 20 (FEI, Eindhoven, Netherlands) microscope equipped with a LaB6 electron source. Images were acquired at an accelerating voltage 200 kV, utilizing the in-built software and a BM Eagle 2K CCD camera (FEI, the Netherlands).

2.8 LMH physical and chemical stability

The physical stability of different formulations was studied by monitoring size, polydispersity index and zeta potential over three months at 4 °C as methods described in the previous section.

2.9 Lovastatin in vitro release study

In vitro LOV release from the LMH, liposome and micelle systems were estimated by a dynamic dialysis membrane diffusion technique using cellulose membrane dialysis tubing (MWCO 14,000; Sigma Aldrich, St. Louis, MO, USA). The dialysis bag was soaked for 2 h before being filled with 10 mL of sample and dipped in a beaker containing the release medium (90 mL) under magnetic stirring (100 rpm). Two release media were investigated, PBS (pH 7.4) - PEG-400 (0.5%) and PBS (pH 7.4)-PEG-400 (0.5%) plus 20% ethanol, both maintained at 37 °C. At predetermined time intervals, a 1 mL aliquot sample was withdrawn from the beaker and replaced with the same volume of fresh release medium. The samples were treated with an equal volume of methanol and sonication (5 min) and then centrifuged at 10,000 rpm (5000 x g) for 10 min to separate the supernatant (LOV). LOV content in the supernatant was determined by diluting 100 μL of each sample with 900 μL of methanol and analysed using HPLC.

2.10 Assessment of cell viability by Alamar Blue method

The cytotoxicity of free drug and LOV-loaded LMH were assessed using a modified Alamar Blue assay. Caco-2 cells were routinely maintained in DMEM with 10% v/v FBS and allowed to grow in a culture flask in an incubator at 37 °C with a controlled atmosphere containing 5% CO_2 and at 95% relative humidity. Cells were passaged at 80–90% confluency at a split ratio of 1:3 using 0.25% trypsin. The cells were seeded into 96-well tissue culture plates at a density of 1×10^4 cells per well in 100 μL of DMEM medium and allowed to attach overnight. LOV-loaded LMH were prepared by dissolving 20 mg of freeze-dried LMH powder (LOV 1.5 mg) with 0.1% DMSO and diluted to the final concentrations of 1.0, 0.5, 0.10, 0.05, 0.01, 0.005 and 0.0001 mg/mL with DMEM + 10% FBS. After 24 h incubation, the cytotoxicity of the LMH system was determined. Alamar Blue® solution was directly added to the medium to prepare a final concentration of 10% in each well. After 4 h of incubation, the absorbance was measured at 570 nm and 596 nm using a Multiskan Ascent plate reader (Thermo Fisher, Waltham, MA, USA). Results were expressed as % cell viability calculated as the absorbance ratio between sample and control (100% viable), which was obtained by incubating cells without any drug.

2.11 Permeability assessment of LOV-LMH in Caco-2 monolayers

To prepare a Caco-2 monolayer suitable for permeability assessment, the cells were seeded at a cell density of approximately 40,500 cells/cm^2 on polycarbonate transwell filters in 24-well polystyrene plates and routinely maintained in DMEM at 37 °C with controlled atmosphere containing 5% CO_2 and 90% relative humidity for 21 d. The culture medium was changed on alternate days, firstly in the basolateral and then in the apical compartment (400 and 600 µL, respectively). At the end of 14 and 21 d of differentiation, integrity of the monolayers was assessed by measuring the transepithelial electrical resistance (TEER) in culture medium using a Millicell ERS-2 Voltohmmeter (Millipore Co., Bedford, MA). TEER measurement is routinely used as an index of monolayer confluence and integrity in cell culture experiments. The final TEER values, expressed as resistance per unit area $\Omega\cdot cm^2$, were calculated by subtracting the blank (filter without cells) resistance from the total resistance and then multiplied with effective membrane area 0.49 cm^2. The control TEER value was taken from the media (DMEM + FBS-10%) without cells; it was < 200 $\Omega\cdot cm^2$ and remained constant for the duration of the experiment. The average TEER value in Caco-2 cell monolayers (CCM) containing media was found to be 1435 ± 139 $\Omega\cdot cm^2$ on the 14th day and 1320 ± 196 $\Omega\cdot cm^2$ on the 21st day. These indicated cells were growing and a complete monolayer was developed by 14 d; at further time points the TEER values plateaued (the 8% decrease observed was not statistically different (ANOVA, p>0.05). All the TEER values were persistently above 305 $\Omega\cdot cm^2$, indicating the integrity of the cell monolayers, as 305 $\Omega\cdot cm^2$ is the minimum limit reported by most previous reports of permeability studies [28].

LOV (100 µM) and LOV containing nanocarriers (100 µM LOV) were dissolved in 0.5% v/v of DMSO and HBSS to prepare experiment samples. After 21 d, the cell culture media (DMEM) were replaced and equilibrated with HBSS buffer (400 µL in the apical wells and 600 µL in the basal wells) for 30 min. HBSS buffer was replaced by samples in the apical (400 µL) or basal (600 µL) wells. Incubation was undertaken for 2 h. After incubation 500 µL of samples were taken from the appropriate wells, depending on the direction of transport (*i.e.*, from the basal well for A-to-B transport or the apical well for B-to-A transport), for an efflux ratio (ER) determination as described in Equation 2.

After treatment, the treating solution was withdrawn, and the cells were washed three times with PBS and lysed using methanol. Samples were quantitatively analysed by HPLC for LOV content. These quantitative determinations of LOV were required prior to the determination of the P_{app} value (Equation 1) and efflux ratio (Equation 2).

Analysis then proceeded to determination of the P_{app} value ER and % permeability of LY from equations 1 and 2 [29].

The apparent LOV permeability (P_{app} x 10^{-6} cm/s) was calculated as follows:

$$P_{app} = \frac{V_R}{A \cdot C_0} \cdot \frac{dMt}{dt} \quad \ldots\ldots\ldots\ldots\ldots\ldots\ldots\ldots\ldots\ldots\ldots\text{Eq. (1)}$$

Where V_R is the volume of the receiving chamber, A the monolayer filter area (cm^2), Co the concentration of the compound initially in the donor compartment and dMt/dt is the rate of drug permeation across the cells.

The efflux ratio (ER) was calculated as the ratio of P_{app} determined in the A-to-B direction to P_{app} determined in the B-to-A direction:

$$\text{ER} = (P_{app}\ \text{B-A}) / (P_{app}\ \text{A-B}) \quad \ldots\ldots\ldots\ldots\ldots\ldots\ldots\ldots\ldots\ldots\ldots\text{Eq. (2)}$$

Where the ratio of the basolateral–apical (secretion) component P_{app} B-A to the apical-basolateral (absorption) component P_{app} A-B was assessed. Theoretically, an ER > 1 suggests the presence of one or various efflux transporters affecting the specific drug tested.

2.12 Evaluation of the Caco-2 cell monolayer integrity using Lucifer Yellow

Integrity of the Caco-2 cell monolayers was evaluated using LY. After removing samples for LOV analysis, the remaining liquid was aspirated from the apical and basal wells. 500 µL of 0.1 mg/mL LY solution was added to the apical wells and 1,000 µL of HBSS to the basal wells, these were then incubated at 37 °C for 60 min. 200 µL aliquots of samples were transferred from the basal wells to a 96 well plate and absorbance measured in a spectrofluorometer with excitation wavelength at 570 nm and emission at 585 nm. The fluorescence for HBSS buffer (as blank to deduct the background value used as a media to prepare the samples) and a 0.1 mg/mL LY solution were also measured. The fluorescence intensity of LY was analysed with a Microplate Fluorescence Reader (Tecan i-control FL600, Bio-Tek, Winooski, VT, USA) using a fluorescence excitation wavelength of 540–570 nm (peak excitation is 570 nm) and fluorescence emission at 580–610 nm (peak emission is 585 nm). A standard curve was prepared from 0.5 to 100 μM LY.

2.13 Transportation and cellular uptake of LOV

For transportation and uptake studies, cells were plated at a density of 40,450 cells/cm^2 onto a 24 mm polycarbonate Transwell filter with 0.4 μm pores and a surface area of 0.7 cm^2. At the beginning of each experiment, the monolayer was washed twice with PBS and pre-equilibrated for 30 min with buffer (HBSS). The LOV, liposomes, micelles and LMH solutions of 400 μL (drug content 100 μM) were added to the apical chambers of the monolayers inserted in each well containing 600 μL HBSS (pH 7.4). The pH conditions were chosen in order to reproduce the physiological pH gradient existing *in vivo* across the small intestinal mucosa. The plate was placed in the incubator at 37 ^{o}C and a 500 μL aliquot sample was taken from the basolateral side at fixed time intervals and replaced by the same amount of transport buffer. At the end of the transport experiment (8 h), samples (100 μL) were also taken from the apical chamber. LOV content was measured by HPLC assay.

Intracellular uptake and accumulation of LOV were assessed at the end of the LOV transport experiment, the treated sample solution was withdrawn, and the cells were washed three times with PBS. Cells of each transwell filter were trypsinized, lysed and diluted with 1 mL of methanol and kept for 24 h at room temperature. The solution was then centrifuged at 10,000 rpm for 10 min and the supernatant analysed for LOV with HPLC.

2.15 Statistical analysis

Statistical analysis was performed using the statistical software package SPSS. Data were expressed as mean ± standard deviation (SD). ANOVA was performed using Microsoft Excel. To identify significant differences, a multiple range test was used to compare each group, and the resulting *P* values for each group indicated in the figures.

3. Results and Discussion

3.1. Preparation and characterisation of the nanocarriers

3.1.1. Micelles

Micellar suspensions (with and without LOV) were prepared using vitamin E d-α-tocopheryl polyethylene glycol 1000 succinate (TPGS), which has been shown to influence Caco-2 cells monolayer permeability by inhibiting P-gp [30]. TPGS micelles showed a diameter of 13 ±1 nm (Table 1) and exhibited no significant change in particle size distribution over time, demonstrating the system stability**.** After loading with LOV, a small reduction in size was observed, in agreement with previous observations of drug loading in micelles [31]. Zeta potential of the micelles (both blank and LOV-loaded) were close to zero as TPGS is a non-ionic surfactant.

Table 1. Characterisation of TPGS micelles, liposomes and LMH (mean ± SD, n = 3) in the presence or absence of LOV loading

Nanocarriers		Particle size (nm)	Polydispersity index (PDI)	Zeta potential (mV)	Drug loading (% w/w)	Encapsulation efficiency (%)
TPGS	Blank	13.0 ± 1	0.25 ± 0.05	-1.41 ± 1.9		
Micelles	Loaded	11.0 ± 0.2	0.13 ± 0.02	-1.26 ± 1.5	2.05± 0.08	72 ± 19
PC/CHO/ DSPG	Blank	107 ± 4	0.229 ± 0.01	-33.0 ± 8.9		
Liposomes	Loaded	94.0 ± 2	0.264 ± 0.01	-42.3 ± 1.1	5.04 ±0.29	92 ± 4
LMH (TFH)		149 ± 2	0.246 ± 0.01	- 46.3 ± 1.9	5.58±0.03	79 ± 5

3.1.2. Liposomes

Liposomes with and without LOV were prepared from a combination of phosphatidylcholine (PC), cholesterol (CHO) and DSPG (1,2-distearoyl-sn-glycero-3-phospho-1'-rac-glycerol, sodium-salt) (molar ratio PC/CHO/DSPG 7:3:2). The negatively charged phospholipid DSPG is commonly used to prepare anionic liposomal formulations and contributes to the negative zeta potential observed for DSPG/PC/CHO liposomes (-33 mV). Zeta potential values higher than 25 mV (either positive or negative), are considered necessary to provide colloidal stability due to electrostatic repulsion [32]. The liposomes remained negatively charged after LOV loading.

The diameter of LOV loaded PC/CHO/DSPG liposomes (94.0 nm) was smaller compared to blank liposomes (107.0 nm) (Table 1**)**. When LOV is dissolved together with the lipid mixture, it is located within the liposomal bilayer, where the acyl chains of DSPG provide a favorable environment. Intercalation of LOV into the bilayer leads to a re-arrangement of the membrane structure and a decrease in ordering of the bilayer. This hypothesis is supported by previous studies [33, 34] where reduction of the liposomal membrane organization order and reduced average particle size of the liposomes was reported. De Paula *et al*. showed decreased bilayer organization with increased local anesthetic concentration, reaching a maximum at the drug water solubility, indicating that partitioning in the membrane is limited by saturation of the aqueous phase [35]. The diameter of PC/CHO/DSPG liposomes was within the small unilamellar vesicles size range (SUV < 200 nm), suggested to be suitable for drug delivery applications [36, 37].

3.1.3. Liposome Micelle Hybrid.

LMH were prepared by combining micelles into liposomes using thin film rehydration (TFH). When the TPGS micelles were assembled into the liposome aqueous core, the LMH diameter increased from 94.0 ± 2 nm to 149 ± 2 nm. LMH are considered to be monodispersed (PDI < 0.3) [38] with a zeta potential of - 46.3 mV (Table 1), suggesting an increase in the fraction of DSPG in the liposome's outer membrane upon incorporation of the micelles. LOV loading was highest for LMH, achieving 5.6%, compared to 2.1% for micelles and 5.0% for liposomes.

Cryo-transmission electron microscopy (Cryo-TEM) images of LMH and liposomes (Fig. 1) displayed a spherical shape surrounded by a lipid bilayer (unilamellar) with an average diameter around 100 nm, in good agreement with dynamic light scattering. Notably, there were some micelles ("worm-like") scattered inside the inner aqueous core of the LMH (Fig. 1b), that were not observed inside the blank liposomes (Fig. 1a).

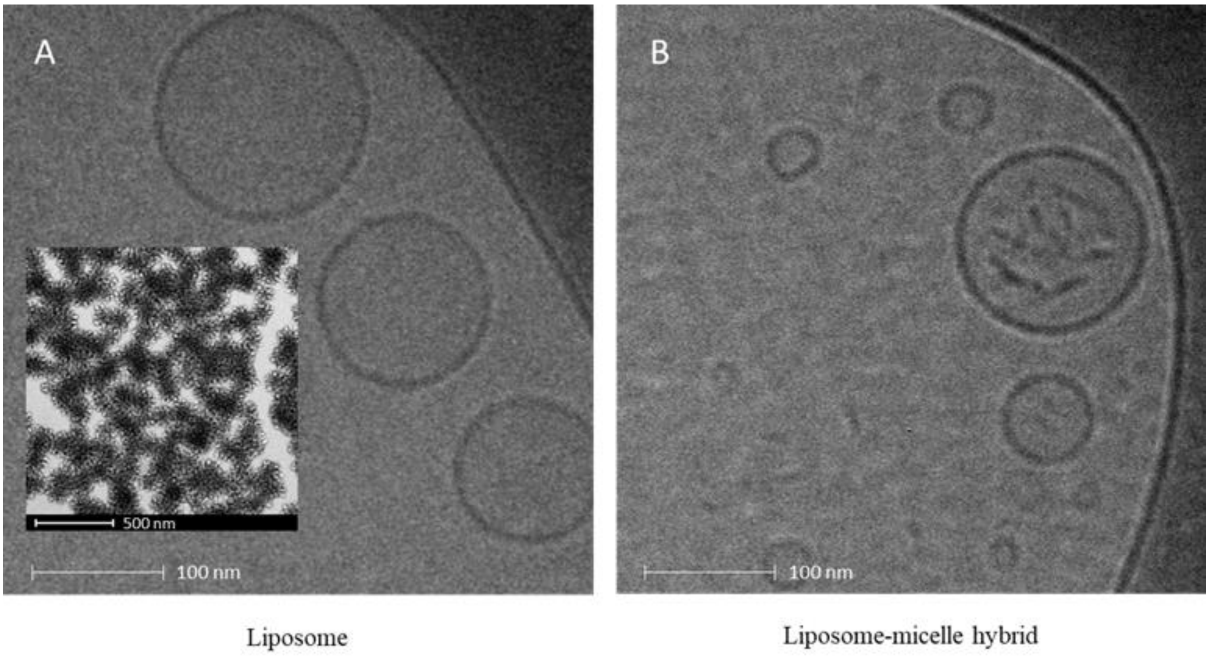

Fig. 1. Cryo-TEM images of a) DSPG/PC/CHO liposomes and b) LMH.

3.2. Physical stability of nanocarriers

Upon storage, liposomes tend to degrade or aggregate and fuse [39], which may lead to drug leakage during storage or after administration. With this in mind, we investigated the stability of LOV-loaded micelles, liposomes and LMH in aqueous dispersions over 3 mos at 4 °C **(**1 mM NaCl). For LOV-loaded micelles, a slight increase in diameter was observed from 11 to 14 nm over the course of time (Table S1). The size of liposomes also increased from 94 to 158 nm. Interestingly, for LMH the size decreased from 168 ± 2 to 134 ± 0.7 nm during storage. The combination of lipids and TPGS demonstrated improved stability, as has been observed for mixed micelles [40].

3.3. LOV release studies

The release kinetics of LOV from micelles, liposomes and LMH were determined *in vitro* at 37 °C using the dialysis bag method [41] and 0.5% PEG400 in PBS as release medium (Fig 2.) (31.63 µg/mL drug dissolved in this buffer)**.**

For micelles, sustained release characteristics were observed, with 40% LOV released within 12 h, followed by a more gradual release to 90% over 240 h (Fig. 2a). This is attributed to micelles restricting the release of LOV, with their hydrophobic core interacting with the hydrophobic LOV. Similar sustained release properties have been reported in the literature for doxorubicin loaded linoleic acid-chitosan copolymer micelles [42].

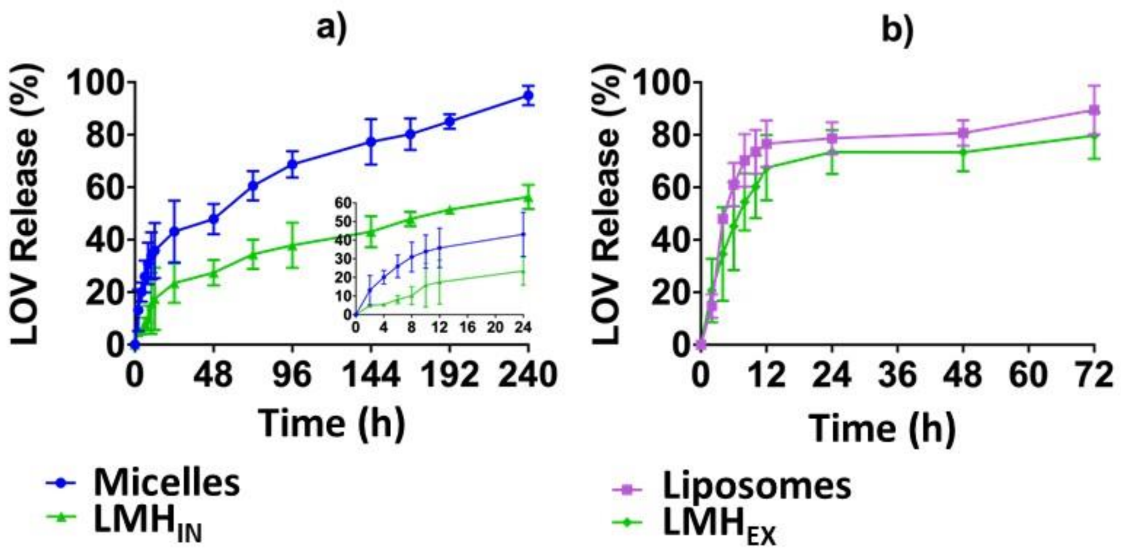

Fig. 2. LOV release from a) micelles and LMH_{IN} (blank lipid bilayer + loaded aqueous inner core) for 24 h (inset graphs) and up to 10 d with (PBS + PEG-400 (0.5%), b) liposomes and LMH_{EX} (loaded lipid bilayer + blank aqueous inner core) at 37 °C in dialysis bag (mean ± SD, n = 3).

From LMH_{IN} (LOV-loaded only within the micelles**)** **(**Fig. 2a), the LOV release was sustained over 10 d and noticeably slower compared to the micelles. Only 17 % (compared to 40% for micelles) of LOV was released within 12 h, followed by sustained release to almost 56% at 240 h (compared to 90% from micelles). In the case of LMH_{IN}, the LOV loaded in micelles has to escape the hydrophobic micellar core and then the liposome bilayer. Therefore, the release rate is slower than for the micelles alone. Moreover, TPGS molecules may affect physicochemical properties and thus stabilize and modify the liposome bilayer structure, which may control the release of the drug.

LOV released from liposomes relatively fast in the first 12 h, with 75% of LOV released at 24 h before plateauing and reaching 85% LOV released after 72 h (Fig. 2b). When LOV was loaded in the lipid bilayer of LMH containing blank micelles (LMH_{EX}), the LOV release profile was similar to that of liposomes. Within 12 h, 67% of LOV was released before plateauing around 73% LOV released at 24 h. The observed retarded LOV release may also be due to TPGS molecules inserting into the liposome bilayer, which has been demonstrated previously for TPGS modified liposomes [43].

Release studies of LOV from micelles, liposomes and LMH (LOV loaded in micelles and lipid bilayer) were performed with the release media of 20% ethanol in water in addition to Tween-80 (0.2% w/v) (Fig. 3). A similar LOV release profile was observed from micelles and liposomes, with approximately 95 % LOV release within 48 h from both nanocarriers (Fig. 3**).** In comparison, retarded release was observed from LMH, with 48% LOV release within 48 h demonstrating a controlled release profile from the hybrid system (Fig. 3). Here, LOV loaded in micelles within the liposome core has provided controlled drug release.

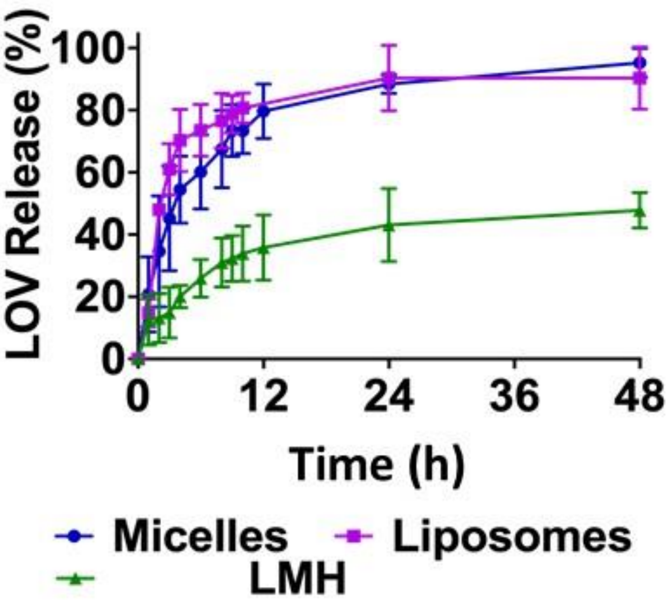

Fig 3. LOV release from micelles, liposomes and LMH (lipid bilayer and aqueous inner core) in release media (PBS with 0.2% of tween 80) and 20 % ethanol at 37 °C in dialysis bag (mean ± SD, n = 3).

Altered LOV release from the nanocarriers was observed in Fig. 3 compared to Fig. 2a and b, due to the different release buffer. It has been reported that the presence of ethanol destabilises the liposomes by penetrating into the liposome lipid bilayer to reversibly decrease its barrier properties [44]. Effect of ethanol in drug release from micelles has not been reported. However, ethanol is reported to have surface active properties that help to swelling the micelles, where for liposomes and hybrid presence of ethanol increases membrane fluidity. Combined with these results suggest that ethanol can lead to increased LOV release from both micelles and liposomes.

3.4. In vitro drug release kinetics

To determine the release mechanism of LOV from micelles, liposomes, and LMH, the Korsmeyer–Peppas [45] model was used (equation (4)).

$$M_t/M_\infty = Kt^n \qquad \text{Eq. (4)}$$

This model generally describes release the fractional release of drug, M_t/M_∞, with time (t) from a drug delivery system where K is a characteristic kinetic constant and n, an exponent coefficient that characterises the mechanism of release. The value of exponent n indicates the different diffusion controlled drug release mechanisms [46].

In order to access more details of the release mechanism, the diffusion coefficient (D) of LOV from each of the nanocarriers was derived using the non-steady-state diffusion model equation (Equation 5) [47];

$$M_t/M_\infty = 4(Dt/\pi\lambda^2)^{1/2} \qquad \text{Eq. (5)}$$

Where, D drug diffusion coefficient at time t, λ is the thickness of the nanocarriers (the value is too small, so it was considered negligible) and t is the time of the measurement.

Table 2**:** The exponent value (n) used to characterise the LOV release mechanism and the diffusion coefficient (D) from the LOV release data for micelles, liposomes and LMH (release media PEG-400, 0.5% and 0.2 % Tween 80 + ethanol).

Nanocarriers	PEG400, 0.5%			Tween 80 + ethanol		
Type	n	R^2	D (m²/s) x 10^{-10}	n	R^2	D (m²/s) x 10^{-10}
Liposome	0.22	0.941	7.96	0.296	0.959	5.79
Micelle	0.347	0.993	3.82	0.337	0.981	5.12
LMH_{EX}	0.528	0.930	5.39	--	--	--
LMH_{IN}	0.286	0.972	1.28	--	--	--
LMH	--	--	--	0.286	0.977	3.18*

*double loaded LMH

According to Korsmeyer and Peppas [45] a value for $n < 0.5$ suggests that the overall diffusion mechanism is Fickian. Here, the values of n were below 0.5 for LMH and other nanocarriers, suggesting the mechanism of LOV release from nanocarriers is Fickian diffusion.

If we consider D (see Table 2) for LOV release in the PBS with PEG400 (0.5%, v/v) media, it was observed that $D_{liposome} > D_{micelle}$, reinforcing the hypothesis that the LOV is interacting with the hydrophobic micellar core and therefore retarding its release. Interestingly, $D_{liposome} > D_{LMHex}$, suggesting that there is material transfer between the micelles and the liposomes, reducing the LOV mobility within the lipid bilayer of the LMH_{EX}. Not surprisingly, $D_{LMHin} < D_{liposome}/ D_{micelle}$, as the LOV must diffuse from the micelles before also having to transit across the liposome bilayer before reaching the release media.

Next, if we consider D (Table 2) for LOV release in the Tween 80/ethanol media, we observe a reduction in $D_{liposome}$ (compared to LOV release in the PEG400 media). This may be due to the interaction of the Tween 80 with the liposome surface, thereby decreasing LOV release. In contrast, we observe an increase in $D_{micelle}$ (again, compared to LOV release in the PEG400 media), which may be due to the ethanol in the media acting as a permeation enhancer. Finally, we observe $D_{LMH} < D_{liposome} \approx D_{micelle}$, which is attributed to the additional barrier to LOV release from micelles within the liposomes to LOV released from reaching the external media (the Tween 80 may also play a role here).

3.5. Caco-2 cell monolayer permeability studies

Biocompatibility of the nanocarriers was tested on Caco-2 cells by an Alamar Blue assay prior to commencement of the permeability assessment. As shown in Fig. S1. LOV-LMH showed no toxic effect on Caco-2 cells at LOV concentrations from 0.0001 to 1 mg/mL, i.e. cell viability was ~100%.

Permeability analysis on Caco-2 cell monolayers was performed on day 21, when they are reported to have well-differentiated and polarized columnar cells with tight junctions and microvilli expression organised as a brush border [48, 49, 50]. TEER values were measured in the presence of LOV encapsulated in micelles, liposomes and LMH as well as free LOV solutions, and ranged from 687 to 1497 $\Omega \cdot cm^2$ (after background resistance was subtracted) in HBSS buffer. At the end of the permeation studies (120 min), these values ranged from 446 to 663 $\Omega \cdot cm^2$ which indicates integrity of the cell monolayer was retained as reported previously [48].

After 2 hours of treatment, the TEER values of cell monolayers was decreased in the presence of micelles, liposomes, LMH and LOV to 55 %, 46 %, 34 % and 90 % of the initial value, respectively (Fig.4). Thus, a greater reduction was observed for LMH than liposomes and micelles. The change in permeability for all nanocarriers was significant compared to LOV (ANOVA, $p<0.05$). From this drop in resistance, we concluded that the nanocarriers were able to open the tight junctions (TJ), increasing paracellular permeability of the Caco-2 cells, as reported by Ward *et al* [51]. The TEER did not change significantly for the control system (no treatment) in HBSS buffer and cells. The findings here correlate with similar decreased TEER values for docosahexaenoic acid and eicosapentaenoic acid-enriched phosphatidylcholine liposomes [52] and risperidone loaded mmePEG750 P(CL-co-TMC) micelles [53].

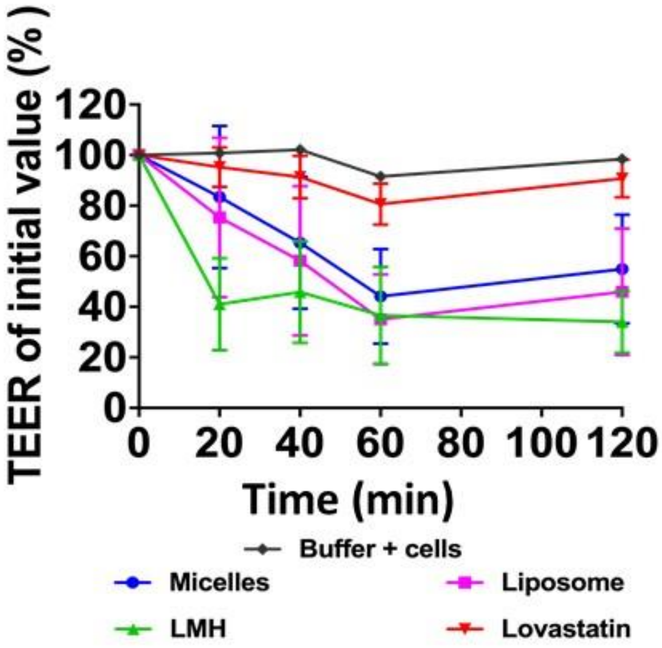

Fig. 4: Effect of 100 µM LOV encapsulated in micelles, liposomes, LMH and free LOV on the TEER in Caco-2 cell monolayers (21 d old) in HBSS over the 2 h treatment period. Control without treatment (cells and buffer only). The data are presented as mean ± SD ($n = 4$). One-way ANOVA analysis indicates statistically significant ($p< 0.05$) difference between control and nanoparticles was 0.006.

The permeation coefficient, or P_{app}, was quantified for bidirectional transport of LOV across the CCM. The P_{app} of LOV across CCM's in the absorptive (apical-to-basolateral; A→B) direction increased by 1.34, 1.23 and 1.14-fold and in the secretory (basolateral-to-apical; B→A) direction by 2.46, 3.53 and 3.33-fold, for LOV encapsulated in micelles, liposomes, and LMH, respectively (Fig. 5). Statistically significant ($p < 0.020$) differences between A→B and B→A permeability for all nanocarriers were observed from single factor ANOVA data analysis. Thus, all the nanocarriers modified the permeability of LOV through the CCM. The enhanced B→A transport vs A→B for *in vitro* permeability of LOV observed here, correlates with previous studies of cerivastatin (3 fold) and of atorvastatin (7 fold higher) (Kivisto *et al.* [54] and Wu *et al.* [55]). It has also been reported by Li *et al*. that statin drugs atorvastatin, LOV, and rosuvastatin, displayed low A→B transport as a result of their low solubility and, as P-gp substrates, they restrict diffusion and transport in the A→B direction compared to the B→A transport [56].

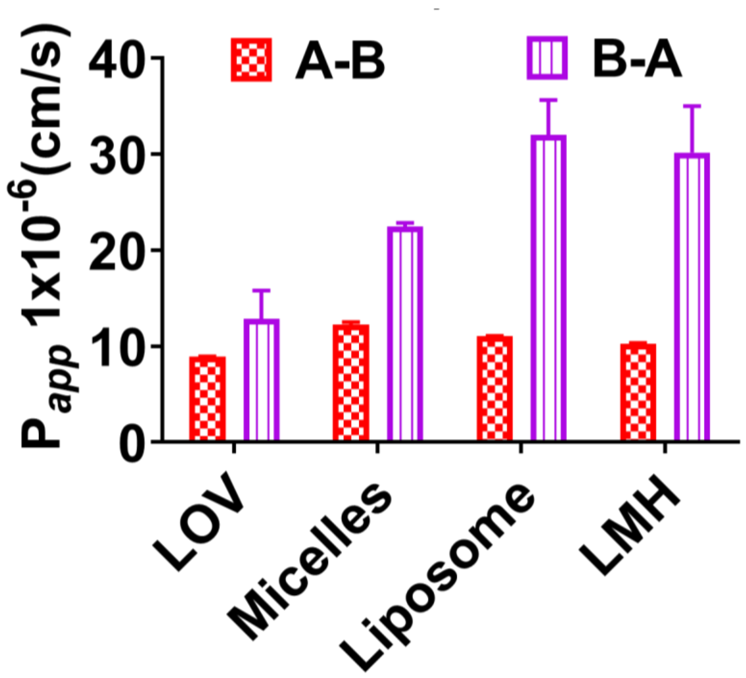

Fig. 5: The A→B and B→A fluxes of LOV and LOV loaded nanocarriers (100 µM) were determined at pH 7.4 as a function of time (2 h at 37°C) and B) Transepithelial efflux of LOV across CCM. Each point represents the mean (4 S.E.M.) of 4 determinations (CCM). One-way ANOVA analysis indicates statistically significant ($P < 0.05$) differences between A→B and B→A permeability was 0.02.

The efflux ratio (ER) is another important parameter used to describe possible mechanisms of drug and nanocarrier permeability. The net flux of LOV was observed in the secretory direction (P_{app} B→A) in CCM (Fig. S2). Theoretically, an ER greater than unity implies the presence of one or various efflux transporters. [57] However, an ER close to 1.0, indicates intestinal absorption to be dominated by passive diffusion [58]. Micelles, liposomes, LMH and free LOV showed an ER ≥ 1 (1.84, 2.90, 2.95, and 1.44, respectively), which confirms transporter mediated diffusion by slowing apical transport and a relative enhancement of the basal pathway.

After the permeability experiments, evaluation of CCM permeability characteristics was performed by measuring the passive passage of LY [52]. LY is a small hydrophilic compound which diffuses through the monolayer mainly via the paracellular space of the tight junctions, [59] and is used as a fluorescent permeability marker with very low permeability (P_{app} < 0.4 X 10^{-6} cm/s) [56]. The results demonstrate that micelles, liposomes, LMH and free LOV were able to increase LY permeability significantly compared to control (buffer and cells only) (Fig. S3) and the difference in LY permeability was not varied among the nanocarriers. This data closely correlates with P_{app} A→B as this study was performed in the A→B direction.

3.6. Cellular transport, intracellular uptake and accumulation

Monitoring the transport of LOV across the CCM, after 8 hours of incubation time, the A→B permeability of LOV loaded in micelles, liposomes and LMH increased approximately 2-fold compared to free LOV (Fig. 6a). In all cases, the transport was biphasic with respect to incubation time: slow transport was detected during the first 2 h of contact (where permeability was assessed, Section 3.5), followed by a steeper increase in transport upon prolonged incubation in the next 6 hours. The transport data showed sigmoidal characteristics over 8 hours for all LOV-nanocarriers including the free LOV and demonstrate the ability of the nanocarriers to enhance LOV transport.

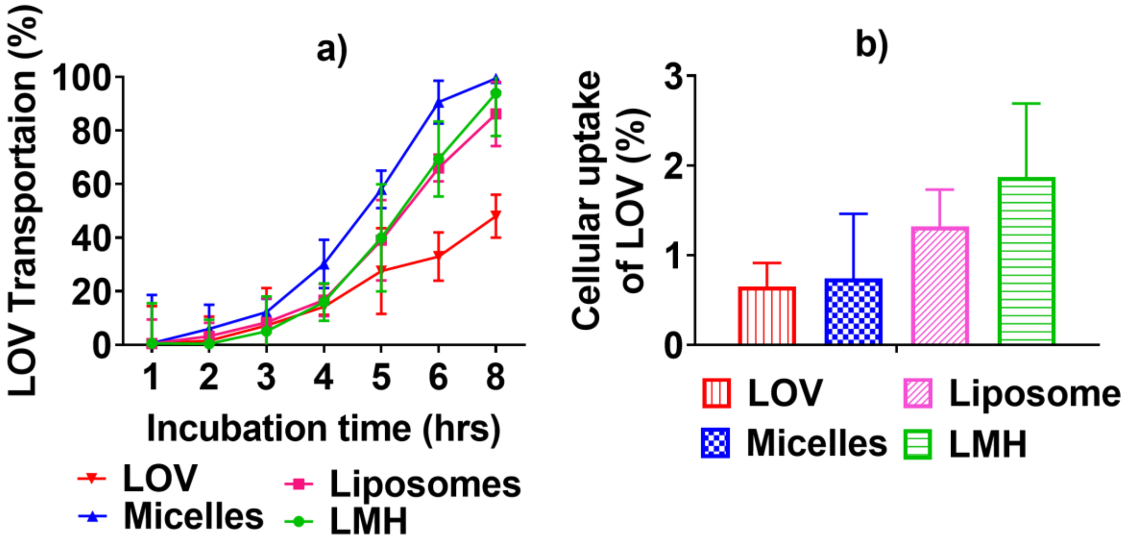

Fig. 6: a) LOV transported across Caco-2 monolayers after 8 hours of incubation in the A→B direction at 37°C in the presence of micelles, liposomes and LMH containing 100 µM of LOV and free LOV 100 µM, expressed as a percentage of the initial concentration of 100 µM LOV, added to the apical compartment, as a function of time, mean ± SD (n=4).b) Caco-2 cell uptake of LOV and LOV loaded nanocarriers (all containing 100 µM LOV). The average size and charge of the nanocarriers, micelles, liposomes, and LMH are shown above the standard deviation bars.

The sigmoidal curve of LOV transport could be explained in the first 2 h of the transport as P-gp mediated at the apical side (A-B) has been shown to limit the transport of LOV through the apical membrane **(**Fig. 6a**)**. After 2 h, LOV transport increased significantly which may result from the saturation of the P-gp present in the apical membrane of the CCM [60] allowing LOV transport to increase. Wang *et al.* reported LOV, atorvastatin and simvastatin are very potent and effective inhibitors of P-gp transport due to their similar molecular structure as well as similar physical and chemical properties [10]. The paracellular mechanism of absorption that improved the permeability of LOV by assisting its transport through the CCM may be explained by the ability of nanocarriers to open up the tight junctions, thus allowing the released drug to permeate via the paracellular route [61]. For micelles, TPGS molecules have been described to be capable of inhibiting the biological activity of P-gp [62] therefore, greater transport was found for micelles as reported by Chen *et al*. [30] and Dintaman *et al.* [63].

At the end of the LOV transport experiment (8 h), the intracellular uptake and accumulation of LOV were assessed to determine which carriers promoted the greater transportation and accumulation of drug molecules inside the cells (Fig. 6b**)**. The Caco-2 cell uptake of LOV encapsulated in micelles, liposomes and LMH were 1.14-fold, 2.03-fold, and 2.88-fold higher than that of LOV at the same concentration (100 µM), respectively, indicating that LOV nanocarriers had a strong influence on uptake and accumulation of LOV in the Caco-2 cell monolayers.

4. Conclusion

A novel LMH system consisting of TGPS micelles encapsulated in liposomes has been developed for delivery of LOV. Compared with the individual micelles and liposomes, LMH has improved LOV loading and aqueous solubility, sustained LOV release, increased permeability and enhanced transport across an epithelial cell monolayer by inhibiting the P-gp that limits absorption of the poorly soluble LOV. The straightforward preparation method of LMH may be amenable to further scale-up. The results highlight the significance of LMH to enhancing oral bioavailability and could open alternative formulation opportunities for oral delivery of poorly soluble drugs. Overall, these results describe a unique hybrid particle system with advanced, controlled drug release properties, which are a promising drug delivery vehicle for further *in vivo* studies and clinical evaluation.

Declaration of Interest

The authors declare no conflict of interest.

Acknowledgements

Financial support of the Australian National Health and Medical Research Council project grant scheme (APP1026382) is gratefully acknowledged. The Australian Research Council (ARC) Discovery Project Grant (DP130101512), ARC Centre of Excellence Grant (CE140100036), ARC Future Fellowship to PT (FT120100101) and the Australian Government for Australian Postgraduate Awards (APA) scholarship with University top-up to support this research to B. Romana. Special Thanks to Associate Professor Fazlul Huq from University of Sydney for donating cells. Dr Gabriela Garrastazu and Dr Celine Heu are acknowledged for the useful discussion and technical support.

References

1. Giliyar C, Fikstad D, Tyavanagimatt S. Challenges and opportunities in oral delivery of poorly water-soluble drugs. Drug Deliv Technol. 2006;6:57-63.

2. Choi YH, Han H-K. Nanomedicines: current status and future perspectives in aspect of drug delivery and pharmacokinetics. Journal of Pharmaceutical Investigation. 2018 2018/01/01;48(1):43-60. doi: 10.1007/s40005-017-0370-4.
3. Pouton CW. Formulation of poorly water-soluble drugs for oral administration: Physicochemical and physiological issues and the lipid formulation classification system. European Journal of Pharmaceutical Sciences. 2006;29(3-4 SPEC. ISS.):278-287.
4. Kumar S, Bhargava D, Thakkar A, et al. Drug carrier systems for solubility enhancement of BCS class II drugs: A critical review [Article]. Critical Reviews in Therapeutic Drug Carrier Systems. 2013;30(3):217-256. doi: 10.1615/CritRevTherDrugCarrierSyst.2013005964.
5. van de Donk NW, Kamphuis MM, Lokhorst HM, et al. The cholesterol lowering drug lovastatin induces cell death in myeloma plasma cells. Leukemia. 2002;16(7):1362-1371.
6. Henwood JM, Heel RC. Lovastatin. A preliminary review of its pharmacodynamic properties and therapeutic use in hyperlipidaemia. Drugs. 1988;36(4):429-454.
7. Lennernäs H, Fager G. Pharmacodynamics and Pharmacokinetics of the HMG-CoA Reductase Inhibitors. Clinical Pharmacokinetics. 1997 1997/05/01;32(5):403-425. doi: 10.2165/00003088-199732050-00005.
8. Chen C-C, Tsai T-H, Huang Z-R, et al. Effects of lipophilic emulsifiers on the oral administration of lovastatin from nanostructured lipid carriers: physicochemical characterization and pharmacokinetics. European Journal of Pharmaceutics and Biopharmaceutics. 2010;74(3):474-482.
9. Jacobsen W, Kirchner G, Hallensleben K, et al. Comparison of Cytochrome P-450-Dependent Metabolism and Drug Interactions of the 3-Hydroxy-3-methylglutaryl-CoA Reductase Inhibitors Lovastatin and Pravastatin in the Liver. Drug Metabolism and Disposition. 1999;27(2):173-179.
10. Wang E-j, Casciano CN, Clement RP, et al. HMG-CoA Reductase Inhibitors (Statins) Characterized as Direct Inhibitors of P-Glycoprotein. Pharmaceutical Research. 2001 2001/06/01;18(6):800-806. doi: 10.1023/A:1011036428972.
11. Bogman K, Peyer A-K, Török M, et al. HMG-CoA reductase inhibitors and P-glycoprotein modulation. British Journal of Pharmacology. 2009 2001/03/01;132(6):1183-1192. doi: 10.1038/sj.bjp.0703920.
12. Romana B, Batger M, Prestidge CA, et al. Expanding the therapeutic potential of statins by means of nanotechnology enabled drug delivery systems. Current Topics in Medicinal Chemistry. 2014;14(9):1182-1193.
13. Yasmin R, Rao S, Bremmell KE, et al. Porous silica-supported solid lipid particles for enhanced solubilization of poorly soluble drugs. AAPS Journal. 2016;18(4):876-885.
14. Beg S, Sandhu PS, Batra RS, et al. QbD-based systematic development of novel optimized solid self-nanoemulsifying drug delivery systems (SNEDDS) of lovastatin with enhanced biopharmaceutical performance [Article]. Drug Delivery. 2015;22(6):765-784. doi: 10.3109/10717544.2014.900154.
15. Yanamandra S, Venkatesan N, Kadajji VG, et al. Proliposomes as a drug delivery system to decrease the hepatic first-pass metabolism: Case study using a model drug. European Journal of Pharmaceutical Sciences. 2014 2014/11/20/;64:26-36. doi: https://doi.org/10.1016/j.ejps.2014.08.008.
16. Sarangi B, Mishra K, Mohanta GP, et al. In vitro-in vivo correlation (IVIVC) of solid lipid nanoparticles loaded with poorly water-soluble drug lovastatin. European Polymer Journal. 2020 2020/01/05/;122:109366. doi: https://doi.org/10.1016/j.eurpolymj.2019.109366.
17. Roger E, Lagarce F, Garcion E, et al. Biopharmaceutical parameters to consider in order to alter the fate of nanocarriers after oral delivery. Nanomedicine. 2010;5(2):287-306.
18. Owen SC, Chan DPY, Shoichet MS. Polymeric micelle stability. Nano Today. 2012 2012/02/01/;7(1):53-65. doi: https://doi.org/10.1016/j.nantod.2012.01.002.

19. Zhang L, Chan JM, Gu FX, et al. Self-Assembled Lipid−Polymer Hybrid Nanoparticles: A Robust Drug Delivery Platform. ACS Nano. 2008 2008/08/26;2(8):1696-1702. doi: 10.1021/nn800275r.
20. Hallan SS, Kaur P, Kaur V, et al. Lipid polymer hybrid as emerging tool in nanocarriers for oral drug delivery. Artificial Cells, Nanomedicine, and Biotechnology. 2016 2016/01/02;44(1):334-349. doi: 10.3109/21691401.2014.951721.
21. Franzè S, UMM, Paola Minghetti, Francesco Cilurzo. Drug-in-micelles-in-liposomes (DiMiL) systems as a novel approach to prevent drug leakage from deformable liposomes. European Journal of Pharmaceutical Sciences. 2019.
22. Mandal B, Bhattacharjee H, Mittal N, et al. Core–shell-type lipid–polymer hybrid nanoparticles as a drug delivery platform. Nanomedicine: Nanotechnology, Biology and Medicine. 2013 2013/05/01/;9(4):474-491. doi: https://doi.org/10.1016/j.nano.2012.11.010.
23. Sezgin Z, Yüksel N, Baykara T. Preparation and characterization of polymeric micelles for solubilization of poorly soluble anticancer drugs. European Journal of Pharmaceutics and Biopharmaceutics. 2006;64(3):261-268.
24. Bangham A, Standish M, Watkins J. Diffusion of univalent ions across the lamellae of swollen phospholipids. Journal of molecular biology. 1965;13(1):238.
25. Bhardwaj U, Burgess DJ. Physicochemical properties of extruded and non-extruded liposomes containing the hydrophobic drug dexamethasone. International journal of pharmaceutics. 2010;388(1):181-189.
26. Mohanraj VJ, Barnes TJ, Prestidge CA. Silica nanoparticle coated liposomes: A new type of hybrid nanocapsule for proteins. International Journal of Pharmaceutics. 2010;392(1-2):285-293.
27. Ong SGM, Chitneni M, Lee KS, et al. Evaluation of Extrusion Technique for Nanosizing Liposomes. Pharmaceutics. 2016;8(4):36. doi: 10.3390/pharmaceutics8040036. PubMed PMID: 28009829; eng.
28. Liang E, Chessic K, Yazdanian M. Evaluation of an accelerated Caco-2 cell permeability model [Article]. Journal of Pharmaceutical Sciences. 2000;89(3):336-345. doi: 10.1002/(SICI)1520-6017(200003)89:3<336::AID-JPS5>3.0.CO;2-M.
29. Zidan AS, Spinks CB, Habib MJ, et al. Formulation and transport properties of tenofovir loaded liposomes through Caco-2 cell model. Journal of liposome research. 2013;23(4):318-326.
30. Chen W, Miao Y-Q, Fan D-J, et al. Bioavailability Study of Berberine and the Enhancing Effects of TPGS on Intestinal Absorption in Rats [journal article]. AAPS PharmSciTech. 2011 June 01;12(2):705-711. doi: 10.1208/s12249-011-9632-z.
31. Liu J, Gong T, Wang C, et al. Solid lipid nanoparticles loaded with insulin by sodium cholate-phosphatidylcholine-based mixed micelles: Preparation and characterization. International Journal of Pharmaceutics. 2007 2007/08/01/;340(1):153-162. doi: https://doi.org/10.1016/j.ijpharm.2007.03.009.
32. Nava G, Piñón E, Mendoza L, et al. Formulation and in vitro, ex vivo and in vivo evaluation of elastic liposomes for transdermal delivery of ketorolac tromethamine [Article]. Pharmaceutics. 2011;3(4):954-970. doi: 10.3390/pharmaceutics3040954.
33. Mura P, Maestrelli F, González-Rodríguez ML, et al. Development, characterization and in vivo evaluation of benzocaine-loaded liposomes. European Journal of Pharmaceutics and Biopharmaceutics. 2007 2007/08/01/;67(1):86-95. doi: http://dx.doi.org/10.1016/j.ejpb.2007.01.020.
34. Cereda S, De Araujo DR, De Paula E. Liposomal prilocaine: preparation, characterization, and in vivo evaluation. Journal of Pharmacy and Pharmaceutical Sciences. 2004.
35. de Paula E, Schreier S. Use of a novel method for determination of partition coefficients to compare the effect of local anesthetics on membrane structure. Biochimica et Biophysica Acta (BBA)-Biomembranes. 1995;1240(1):25-33.

36. Akbarzadeh A, Rezaei-Sadabady R, Davaran S, et al. Liposome: classification, preparation, and applications. Nanoscale Research Letters. 2013;8(1):102. PubMed PMID: doi:10.1186/1556-276X-8-102.
37. Maurer N, Fenske DB, Cullis PR. Developments in liposomal drug delivery systems. Expert opinion on biological therapy. 2001;1(6):923-947.
38. Hope MJ, Nayar R, Mayer LD, et al. Reduction of liposome size and preparation of unilamellar vesicles by extrusion techniques. Liposome technology. 1993;1:123-139.
39. Takeuchi H, Yamamoto H, Toyoda T, et al. Physical stability of size controlled small unilameller liposomes coated with a modified polyvinyl alcohol. International Journal of Pharmaceutics. 1998;164(1–2):103-111. doi: 10.1016/s0378-5173(97)00404-3.
40. Vakil R, Kwon GS. Poly(ethylene glycol)-b-Poly(ε-caprolactone) and PEG-Phospholipid Form Stable Mixed Micelles in Aqueous Media. Langmuir. 2006 2006/11/01;22(23):9723-9729. doi: 10.1021/la061408y.
41. Kono K, Nakai R, Morimoto K, et al. Thermosensitive polymer-modified liposomes that release contents around physiological temperature. Biochimica et Biophysica Acta (BBA) - Biomembranes. 1999 1/12/;1416(1–2):239-250. doi: http://dx.doi.org/10.1016/S0005-2736(98)00226-0.
42. Du Y-Z, Wang L, Yuan H, et al. Preparation and characteristics of linoleic acid-grafted chitosan oligosaccharide micelles as a carrier for doxorubicin. Colloids and Surfaces B: Biointerfaces. 2009;69(2):257-263.
43. Li J, Cheng X, Chen Y, et al. Vitamin E TPGS modified liposomes enhance cellular uptake and targeted delivery of luteolin: An in vivo/in vitro evaluation. International Journal of Pharmaceutics. 2016 2016/10/15/;512(1):262-272. doi: https://doi.org/10.1016/j.ijpharm.2016.08.037.
44. Kuo-Sheng L, Chih-Jen W, Tzu-Chen Y, et al. Combined strategies of apomorphine diester prodrugs and nanostructured lipid carriers for efficient brain targeting. Nanotechnology. 2012;23(9):095103.
45. Korsmeyer RW, Gurny R, Doelker E, et al. Mechanisms of solute release from porous hydrophilic polymers. International journal of pharmaceutics. 1983;15(1):25-35.
46. Singhvi G, Singh M. Review: in-vitro drug release characterization models. Int J Pharm Stud Res. 2011;2(1):77-84.
47. Sutton S, Campbell NL, Cooper AI, et al. Controlled Release from Modified Amino Acid Hydrogels Governed by Molecular Size or Network Dynamics. Langmuir. 2009 2009/09/01;25(17):10285-10291. doi: 10.1021/la9011058.
48. Srinivasan B, Kolli AR, Esch MB, et al. TEER measurement techniques for in vitro barrier model systems. Journal of laboratory automation. 2015 01/13;20(2):107-126. doi: 10.1177/2211068214561025. PubMed PMID: PMC4652793.
49. Violante GD, Zerrouk N, Richard I, et al. Short Term Caco-2/TC7 Cell Culture: Comparison between of Conventional 21-d and a Commercially Available 3-d System. Biological and Pharmaceutical Bulletin. 2004;27(12):1986-1992. doi: 10.1248/bpb.27.1986.
50. Sambuy Y, De Angelis I, Ranaldi G, et al. The Caco-2 cell line as a model of the intestinal barrier: influence of cell and culture-related factors on Caco-2 cell functional characteristics. Cell Biology and Toxicology. 2005 2005/01/01;21(1):1-26. doi: 10.1007/s10565-005-0085-6.
51. Ward PD, Tippin TK, Thakker DR. Enhancing paracellular permeability by modulating epithelial tight junctions. Pharmaceutical Science & Technology Today. 2000 2000/10/01/;3(10):346-358. doi: https://doi.org/10.1016/S1461-5347(00)00302-3.
52. Hossain Z, Kurihara H, Hosokawa M, et al. Docosahexaenoic acid and eicosapentaenoic acid-enriched phosphatidylcholine liposomes enhance the permeability, transportation and uptake of phospholipids in Caco-2 cells. Molecular and cellular biochemistry. 2006;285(1):155-163.

53. Mathot F, van Beijsterveldt L, Préat V, et al. Intestinal uptake and biodistribution of novel polymeric micelles after oral administration. Journal of Controlled Release. 2006;111(1–2):47-55. doi: 10.1016/j.jconrel.2005.11.012.
54. Kivistö KT, Zukunft J, Hofmann U, et al. Characterisation of cerivastatin as a P-glycoprotein substrate: studies in P-glycoprotein-expressing cell monolayers and mdr1a/b knock-out mice [journal article]. Naunyn-Schmiedeberg's Archives of Pharmacology. 2004 August 01;370(2):124-130. doi: 10.1007/s00210-004-0948-z.
55. Wu X, Whitfield LR, Stewart BH. Atorvastatin transport in the Caco-2 cell model: Contributions of P- glycoprotein and the proton-monocarboxylic acid co-transporter. Pharmaceutical Research. 2000;17(2):209-215.
56. Li J, Volpe DA, Wang Y, et al. Use of transporter knockdown caco-2 cells to investigate the in vitro efflux of statin drugs. Drug Metabolism and Disposition. 2011;39(7):1196-1202.
57. Marsousi N, Doffey-Lazeyras F, Rudaz S, et al. Intestinal permeability and P-glycoprotein-mediated efflux transport of ticagrelor in Caco-2 monolayer cells [Article]. Fundamental and Clinical Pharmacology. 2016;30(6):577-584. doi: 10.1111/fcp.12219.
58. Wang Q, Kuang Y, Song W, et al. Permeability through the Caco-2 cell monolayer of 42 bioactive compounds in the TCM formula Gegen-Qinlian Decoction by liquid chromatography tandem mass spectrometry analysis. Journal of Pharmaceutical and Biomedical Analysis. 2017 2017/11/30/;146(Supplement C):206-213. doi: https://doi.org/10.1016/j.jpba.2017.08.042.
59. Fenyvesi F, Kiss T, Fenyvesi É, et al. Randomly methylated β - cyclodextrin derivatives enhance taxol permeability through human intestinal epithelial Caco - 2 cell monolayer. Journal of pharmaceutical sciences. 2011;100(11):4734-4744.
60. Lo Y-L. Phospholipids as multidrug resistance modulators of the transport of epirubicin in human intestinal epithelial Caco-2 cell layers and everted gut sacs of rats. Biochemical Pharmacology. 2000 2000/11/01/;60(9):1381-1390. doi: https://doi.org/10.1016/S0006-2952(00)00451-2.
61. Roger E, Lagarce F, Garcion E, et al. Biopharmaceutical parameters to consider in order to alter the fate of nanocarriers after oral delivery. Nanomedicine. 2010;5(2):287-306.
62. Yu L, Bridgers A, Polli J, et al. Vitamin E-TPGS Increases Absorption Flux of an HIV Protease Inhibitor by Enhancing Its Solubility and Permeability1 [journal article]. Pharmaceutical Research. 1999 December 01;16(12):1812-1817. doi: 10.1023/a:1018939006780.
63. Dintaman JM, Silverman JA. Inhibition of P-glycoprotein by D-α-tocopheryl polyethylene glycol 1000 succinate (TPGS) [Article]. Pharmaceutical Research. 1999;16(10):1550-1556. doi: 10.1023/A:1015000503629.

Supplementary Figures

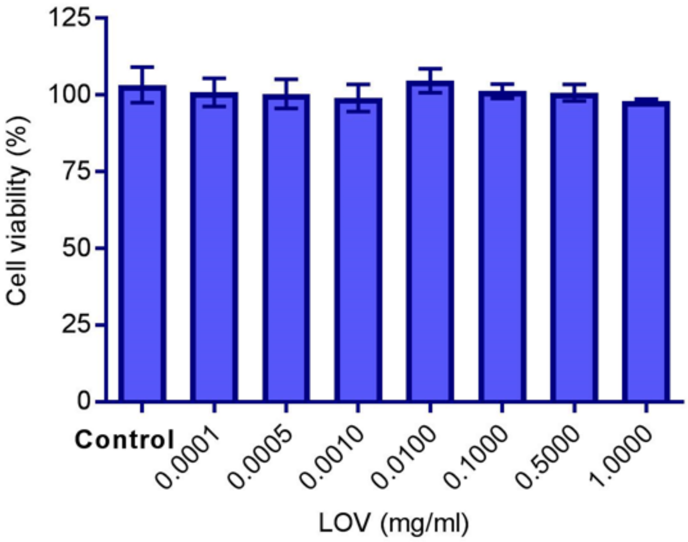

Fig. S1. Caco-2 cell viability as a function of various levels of LOV-LMH inclusion. Viability determined after 48 hours of treatment by Alamar Blue assay. Data presented as the mean ± SD (n = 4) from two individual experiments in quadruplicate. **control without the drug.

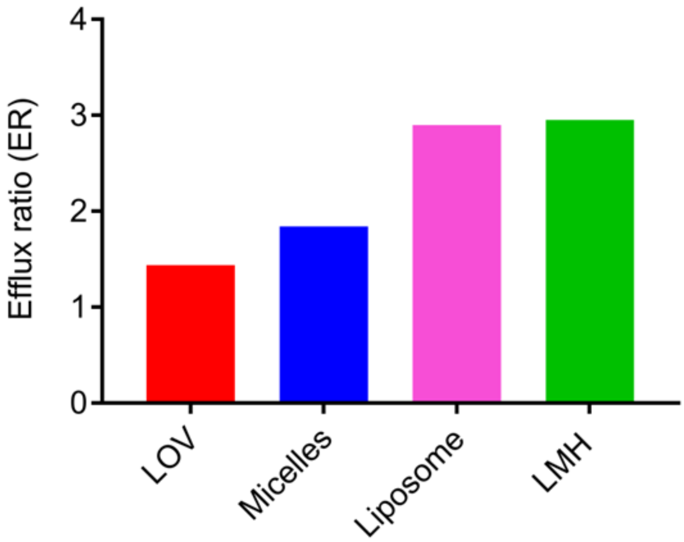

Fig. S2. Efflux ratio of LOV, and LOV incorporated in micelles, liposomes and LMH. as calculated as the ratio of P*app* measured in the B→A direction divided by the P*app* in the A→B direction.

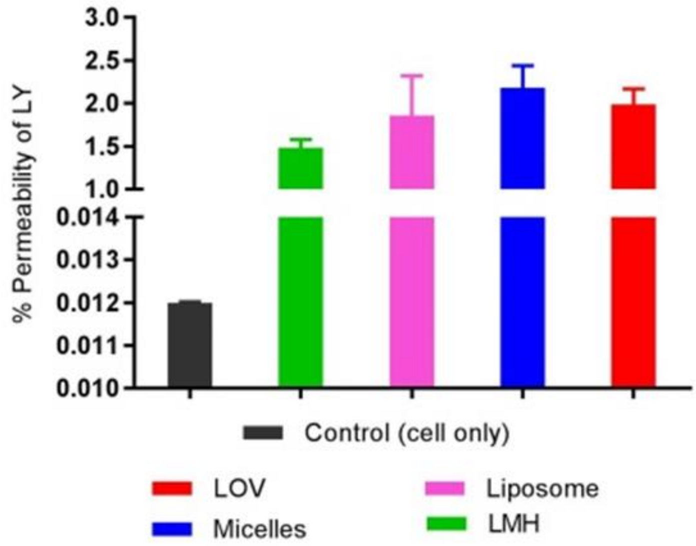

Fig. S3. Percent permeability of LY (100 µM) from A→B; added to the apical chamber of CCM treated with 100 µM LOV and 100 µM LOV incorporated into each nanocarrier; micelles, liposomes, and LMH; were incubated for 1 h with LY. After 1 h samples were collected from the basal chamber. Results are mean ± SD (n = 4).